

Supporting Information for

Tris(8-hydroxyquinoline-5-sulphonate)aluminum intercalated Mg–Al Layered Double Hydroxide with Blue Luminescence by Hydrothermal Synthesis

Shuangde Li,^a Jun Lu,^{a*} Min Wei,^a David G. Evans,^a and Xue Duan^a

^a State Key Laboratory of Chemical Resource Engineering, Beijing University of Chemical Technology, Beijing 100029, P. R. China.

List of Content

1. Structural and compositional characterization of DDS–AQS(x%)/LDHs

Figure S1. Powder XRD patterns of DDS–AQS(x%)/LDHs with various AQS concentration (x).

Figure S2. FT-IR spectra of DDS–AQS(x%)/LDHs.

Figure S3. TG/DTA data for DDS–AQS(x%)/LDHs.

2. Optical properties of DDS–AQS(x%)/LDHs

Figure S4. The solid UV-vis absorption spectra of DDS–AQS(x%)/LDHs with different concentration

Figure S5. The photoluminescence spectra of Na₃AQS (5×10⁻⁵ mol·L⁻¹) aqueous solution with the excitation at 360 nm.

Figure S6. Fluorescence decay curves and the residual plots of the biexponential fits for DDS–AQS(66.67%)/LDHs powder.

Figure S7. The photoluminescence spectra of DDS–AQS(66.67%)/LDH and Na₃AQS film with the excitation at 360 nm.

3. Intercalated structure of AQS anions

Figure S8. ¹H NMR spectrum of Na₃AQS in DMSO-*d*₆ solution at 27 °C.

Figure S9. ¹³C NMR spectrum of Na₃AQS in DMSO-*d*₆ solution at 27 °C.

Figure S10. ¹H–¹H COSY spectrum of Na₃AQS in DMSO-*d*₆ solution at 27 °C.

Figure S11. ¹³C–¹H COSY spectrum of Na₃AQS in DMSO-*d*₆ solution at 27 °C.

Figure S12. The ¹³C NMR assignments of *meridional* AQS based on DFT calculation.

Figure S13. The FT-IR spectra for Na₃AQS and DDS–AQS(66.67%)/LDHs.

1. Structural and compositional characterization of DDS–AQS(*x*%)/LDHs

The XRD patterns of DDS–AQS(*x*%)/LDHs samples are shown in Fig. S1A. The basal spacing of DDS–AQS(*x*%)/LDHs expands firstly from 22.93 Å (*x* = 0) to the maximum (23.88 Å, *x* = 16.67), and then decreases gradually to the minimum (20.50 Å, *x* = 98.04) which can be observed from Fig. S1B. The variation of the interlayer spacing can be attributed to the different arrangements of interlayer guest molecules with different ratios of AQS and DDS anions. The two compounds have been successfully intercalated into the interlayer region which is in accordance with the results of FT-IR spectra shown in Fig. S2. The absorption peaks at 2924 cm^{−1} and 2854 cm^{−1} are assigned to $\nu_{as}\text{CH}_2$ and $\nu_s\text{CH}_2$ vibration of DDS, the intensities are decreasing with the increased proportion of AQS from 0 to 0.9803. However those at 1580 cm^{−1} and 1502 cm^{−1} are characteristic of the $\nu\text{C}=\text{C}$ mode of pyridine ring, their intensities are increasing with the *x* varying from 0 to 0.9803. This can manifest the AQS anions are quantitatively co-intercalated into the interlayer of LDHs with the surfactant DDS.

The chemical compositions of DDS–AQS(*x*%)/LDHs listed in Table 1 were calculated as follows: The percentages of C, N, and H in the samples were obtained by CHN elemental analysis. According to the measured percentage of N, which is present exclusively in the AQS anion, the molar amount of AQS can be determined, and thus the amounts of C, S, and Al contributed by AQS can be obtained. On the other hand, the molar ratios of Mg to Al and Mg to S can be calculated from the ICP-AES results. Therefore, simultaneous equations can be established according to the charge balance relationship between host and guest, and the fact that different guest species contribute to the total content of C. Solution of these equations gives the molar amount of each guest species. Furthermore, the molar amount of water can be obtained from the thermogravimetric-differential thermal analysis (TG-DTA) curve or calculated from the measured percentage of H, once the amounts of interlayer guest anions are known.

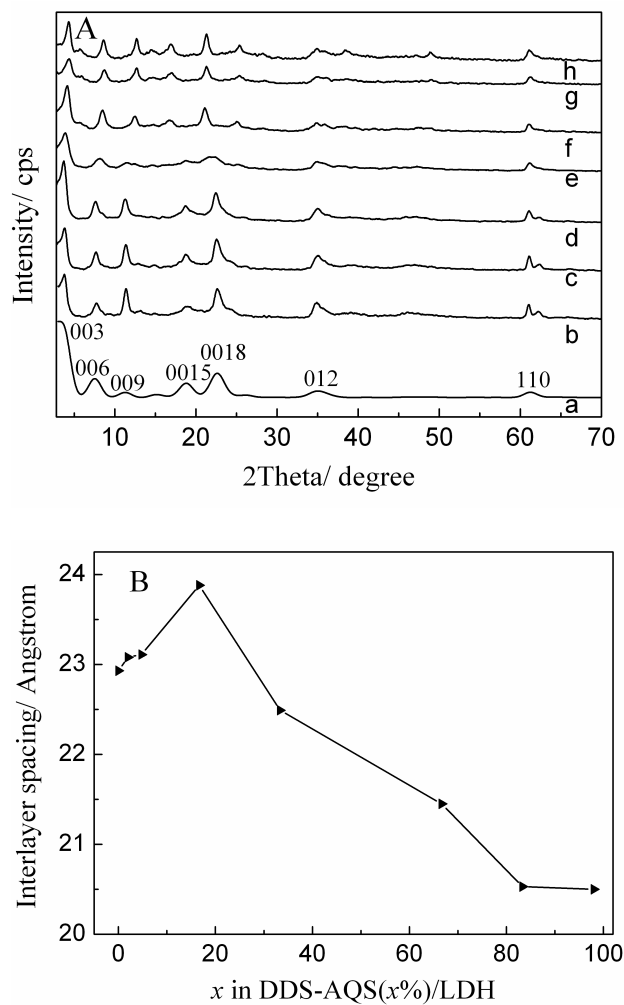


Figure S1. A) Powder XRD patterns of DDS–AQS($x\%$)/LDHs. ($x = a, 0$; $b, 1.96$; $c, 4.76$; $d, 16.67$; $e, 33.33$; $f, 66.67$; $g, 83.33$; $h, 98.04$). B) The plots of interlayer spacing vs AQS anions concentration.

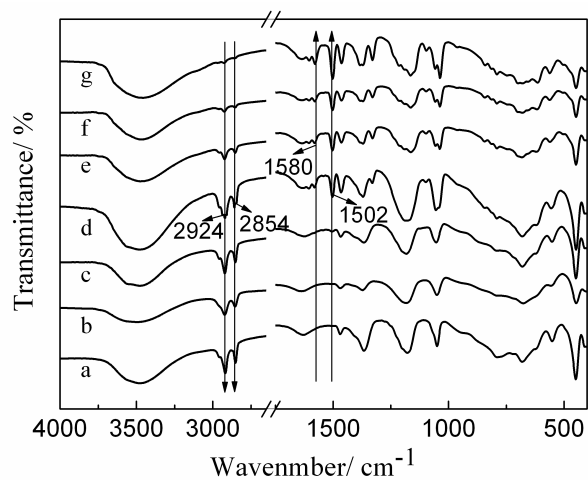


Figure S2. FT-IR spectra of DDS–AQS($x\%$)/LDHs. ($x = a, 0$; $b, 4.76$; $c, 16.67$; $d, 33.33$; $e, 66.67$; $f, 83.33$; $g, 98.04$).

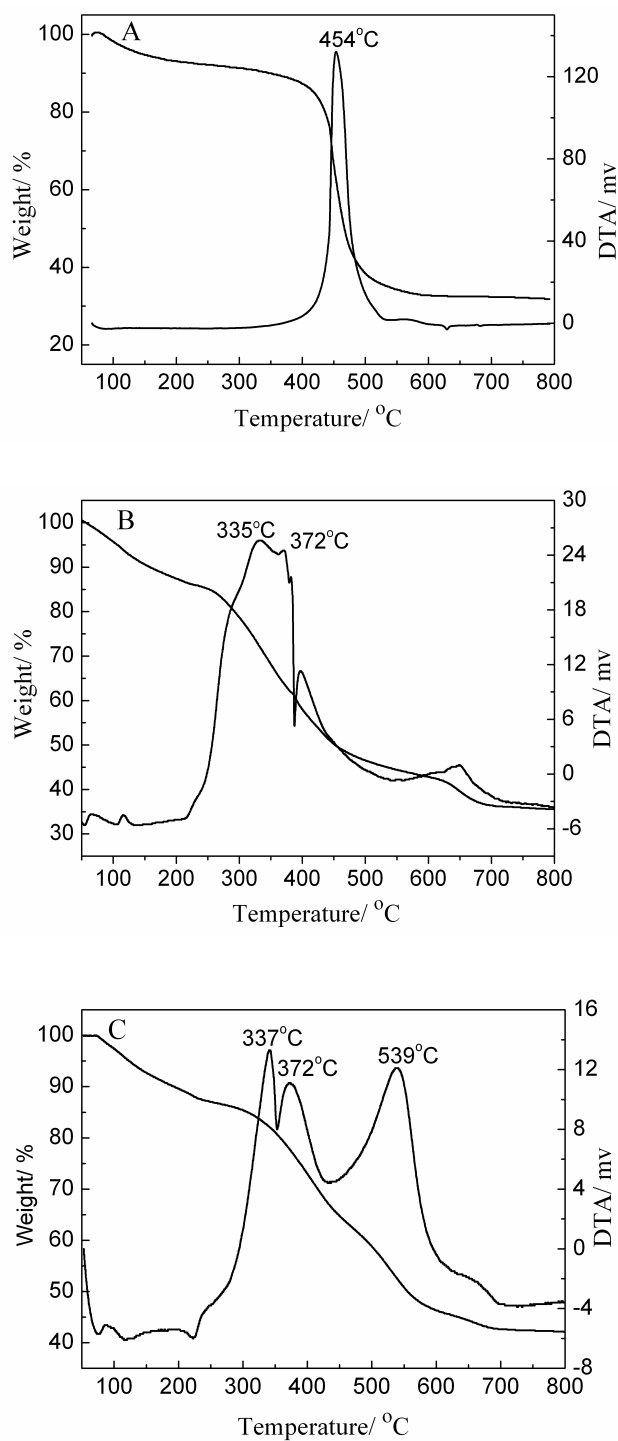


Figure S3. TG/DTA data for DDS–AQS($x\%$)/LDHs.
A) Na₃AQS. B) DDS/LDHs. C). DDS–AQS(66.67%)/LDHs

For DDS/LDHs, three distinct weight loss stages were observed in the TG-DTA curve (Fig. S3B). The first step is attributed to the removal of surface-adsorbed water and interlayer water up to about 180 °C and dehydroxylation of the host layers up to

290 °C. Another in the 290 – 400 °C range corresponds to the decomposition of DDS. For DDS-AQS(66.67%)/LDHs, the two exothermic peaks at 337 and 372 °C are similar to curve Fig. S3B and are the decomposition of DDS, the third exothermic peak at 539 °C is due to the decomposition of AQS anions.

2. Optical properties of DDS–AQS($x\%$)/LDHs

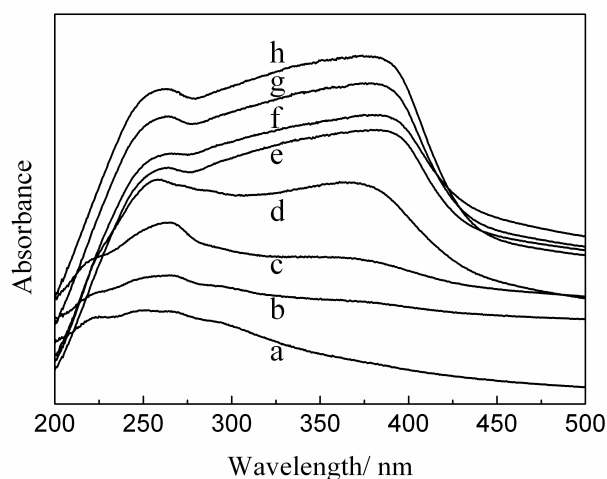


Figure S4. The solid UV-vis absorption spectra of DDS–AQS($x\%$)/LDHs. ($x = a, 0$; $b, 1.96$; $c, 4.76$; $d, 16.67$; $e, 33.33$; $f, 66.67$; $g, 83.33$; $h, 98.04$).

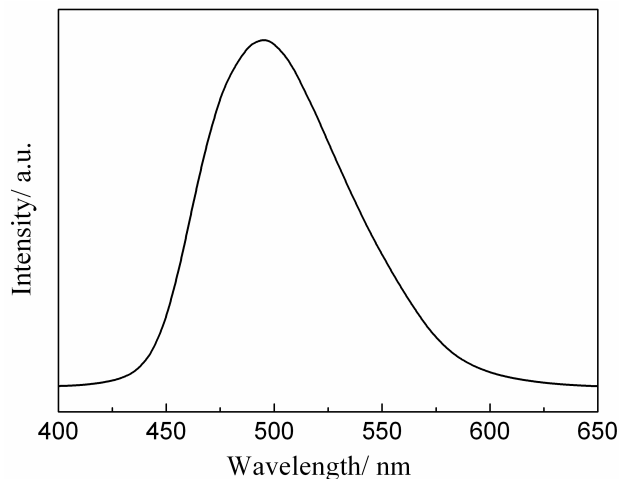


Figure S5 The photoluminescence spectra of Na_3AQS ($5 \times 10^{-5} \text{ mol} \cdot \text{L}^{-1}$) aqueous solution with the excitation at 360 nm.

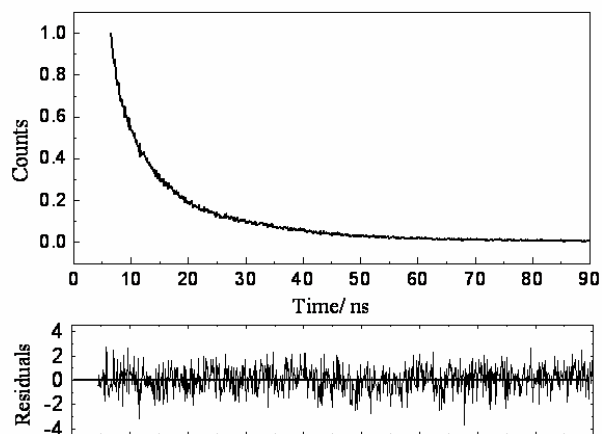


Figure S6. Fluorescence decay curve and residual plots of fits with biexponential for DDS–AQS(66.67%)/LDHs powder.

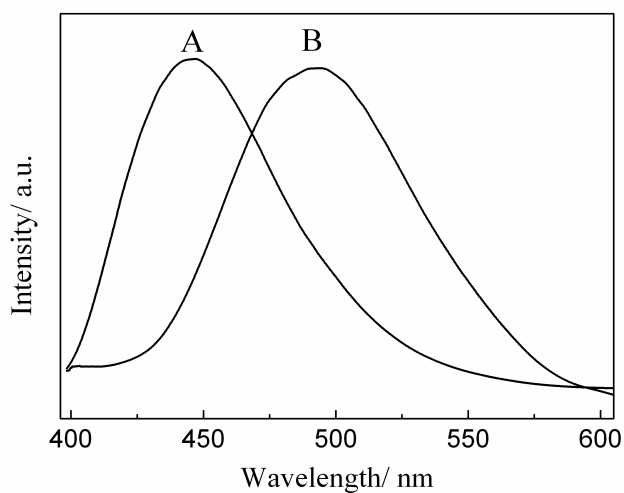


Figure S7. The photoluminescence spectra of A) DDS–AQS(66.67%)/LDHs film and B) Na_3AQS film with the excitation at 360 nm.

3. Intercalated structure of AQS anions

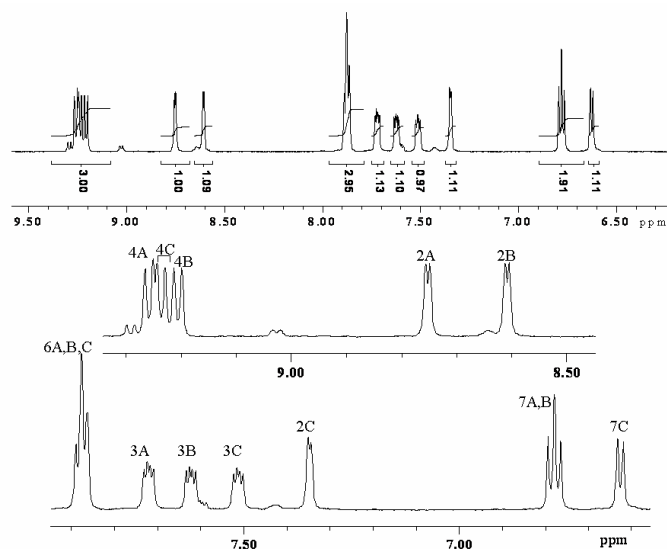


Figure S8. ^1H NMR spectrum of Na_3AQS in $\text{DMSO-}d_6$ solution at $27\text{ }^\circ\text{C}$. The expanded spectrum is also shown and the integrated peak intensities are given by black figures.

The assignments of the resonance lines are based on the ^1H – ^1H COSY experiments in Figures S10 and the literature [1]. We carry out a complete assignment of resonance lines according to the known data except H6 and H7.

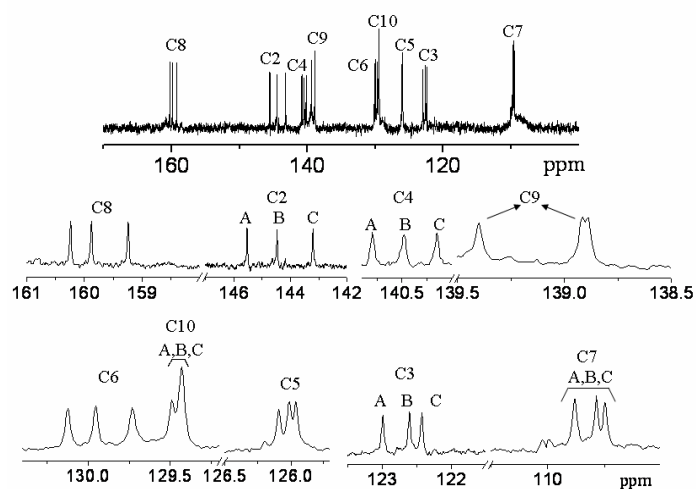


Figure S9. ^{13}C NMR spectrum of Na_3AQS in $\text{DMSO-}d_6$ solution at $27\text{ }^\circ\text{C}$. The expanded spectrum is also shown.

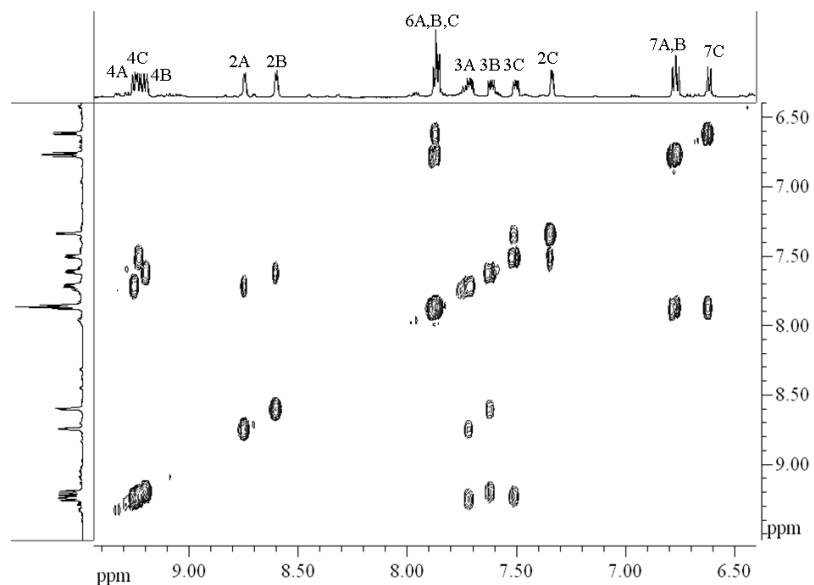


Figure S10. ^1H – ^1H COSY spectrum of Na_3AQs in $\text{DMSO-}d_6$ solution at $27\text{ }^\circ\text{C}$.

H_2C resonance lines are significantly separated from H_2A and H_2B resonance lines. This unequally spaced resonance line splitting maybe is due to the different environment of the three H_2 hydrogen atoms. The DFT calculation reveals that the H_2C hydrogen is located near the nitrogen atoms in the adjacent sulfoquinoline ring, whereas the H_2A and H_2B hydrogen atoms are located near the oxygen atoms. That is, the local environments of the H_2A and H_2B atoms are similar, whereas that of the H_2C hydrogen is quite different. The similar phenomenon is also reported by Kaji [2].

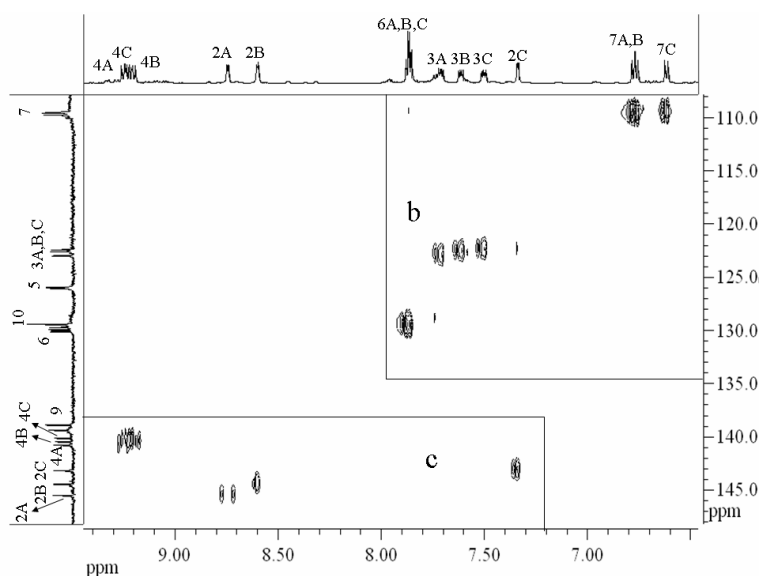


Figure S11(a) ^{13}C – ^1H COSY spectrum of Na_3AQs in $\text{DMSO-}d_6$ solution at $27\text{ }^\circ\text{C}$.

Based on the solution ^1H NMR spectrum, the assignments of solution ^{13}C NMR resonance lines are carried out. The assignments of non-protonated C5, C8, C9, C10 carbon atoms are empirically carried out by considering that the C5 is bonded to sulfonic group, the C8 is bonded to oxygen atom and the C9 is bonded to nitrogen atom. The DFT calculation also confirms the assignments of the ^{13}C NMR including these non-protonated carbon atoms (see Figures S12).

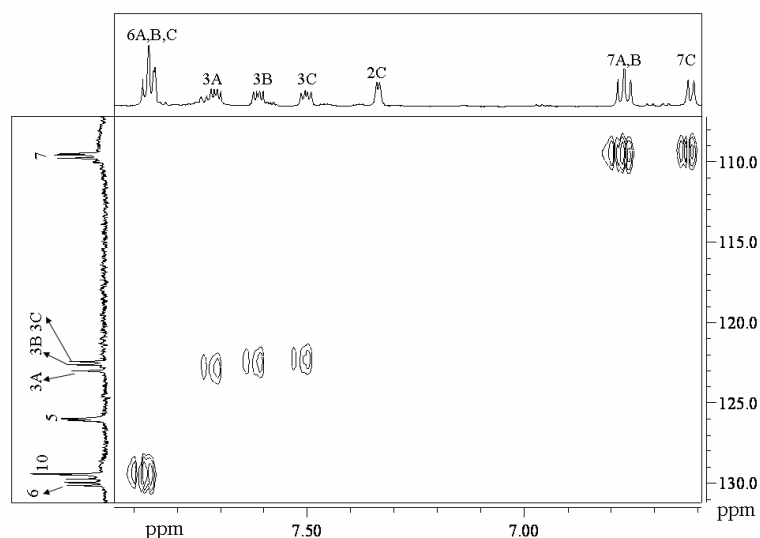


Figure S11(b). The expanded ^{13}C – ^1H COSY spectrum of Na_3AQs in $\text{DMSO-}d_6$ solution at $27\text{ }^\circ\text{C}$, which corresponds to the rectangular region (b) in Figure S11(a).

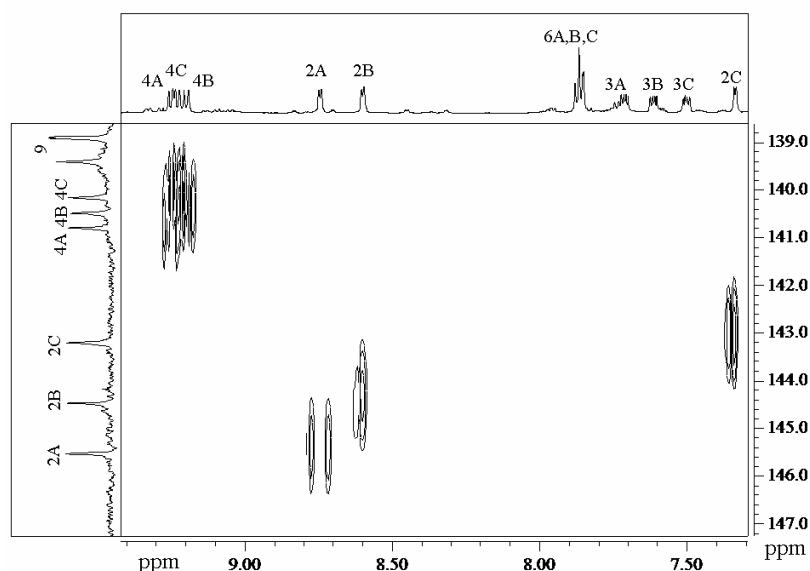


Figure S11(c). The expanded ^{13}C – ^1H COSY spectrum of Na_3AQs in $\text{DMSO-}d_6$ solution at $27\text{ }^\circ\text{C}$, which corresponds to the rectangular region (c) in Figure S11(a).

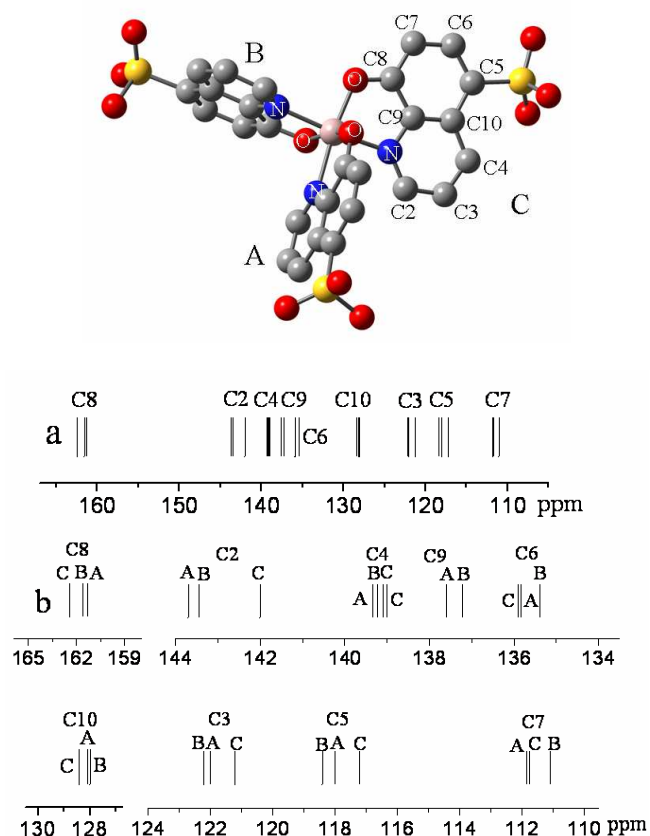


Figure S12. a) The assignments of ^{13}C NMR spectrum for *meridional* AQS molecule based on DFT calculation (the letters, A, B, and C correspond to the three ligands of the AQS model at the top). The expanded spectra are shown in (b). The hydrogen atoms are omitted for clarity.

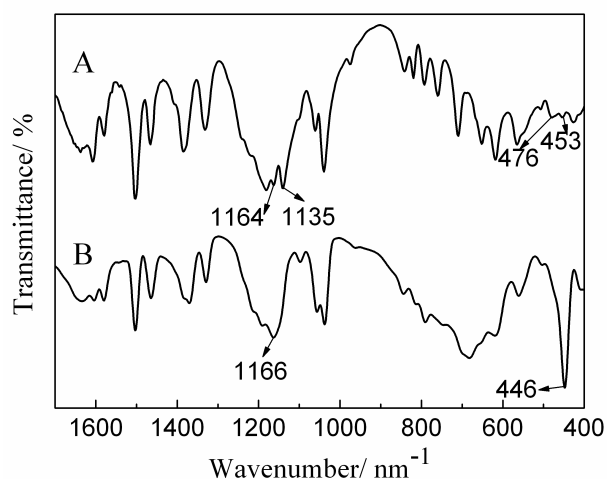


Figure S13. FT-IR spectra for A) Na_3AQS powder and B) $\text{DDS-AQS}(66.67\%)/\text{LDHs}$.

References:

- [1] F. Camerel, J. Barbera, J. Otsuki, T. Tokimoto, Y. Shimazaki, L.-Y. Chen, S.-H. Liu, M.-S. Lin, C.-C. Wu, R. Ziessel, *Adv. Mater.* **2008**, *20*, 3462.
- [2] H. Kaji, Y. Kusaka, G. Onoyama, F. Horii, *J. Am. Chem. Soc.* **2006**, *128*, 4292.